



**HAL**  
open science

# New prediction interval and band in the nonlinear regression model: Application to predictive modelling in food science

Jean-Pierre Gauchi, Jean-Pierre Vila, Louis Coroller

## ► To cite this version:

Jean-Pierre Gauchi, Jean-Pierre Vila, Louis Coroller. New prediction interval and band in the non-linear regression model: Application to predictive modelling in food science. *Communications in Statistics - Simulation and Computation*, 2009, 39 (02), pp.322-334. 10.1080/03610910903448799 . hal-00550610

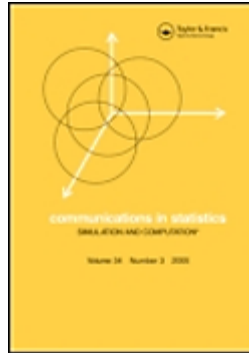
**HAL Id: hal-00550610**

**<https://hal.science/hal-00550610>**

Submitted on 29 Dec 2010

**HAL** is a multi-disciplinary open access archive for the deposit and dissemination of scientific research documents, whether they are published or not. The documents may come from teaching and research institutions in France or abroad, or from public or private research centers.

L'archive ouverte pluridisciplinaire **HAL**, est destinée au dépôt et à la diffusion de documents scientifiques de niveau recherche, publiés ou non, émanant des établissements d'enseignement et de recherche français ou étrangers, des laboratoires publics ou privés.



**New prediction interval and band in the nonlinear regression model: Application to predictive modelling in food science**

Journal:	<i>Communications in Statistics - Simulation and Computation</i>
Manuscript ID:	LSSP-2007-0136.R2
Manuscript Type:	Original Paper
Date Submitted by the Author:	14-Oct-2009
Complete List of Authors:	GAUCHI, Jean-Pierre; INRA, MIA(UR341) VILA, Jean-Pierre; INRA, LASB COROLLER, Louis; UBO, LUMAQ
Keywords:	Prediction interval, Prediction band, Nonlinear regression, Parametric confidence region, Predictive modelling, Food Science
Abstract:	We propose a new prediction interval and band for the nonlinear regression model. The construction principle of this interval and band is based on an exact confidence region for parameters of the nonlinear regression model. This region, fully described in Vila & Gauchi (2007), provides a rigorous justification for the new prediction interval and band that we propose. This new band is then compared to the classical bands, and also to the band based on the bootstrap resampling method. The comparison of these bands is undertaken with simulated and real data from predictive modelling in food science.
Note: The following files were submitted by the author for peer review, but cannot be converted to PDF. You must view these files (e.g. movies) online.	
revisedarticle.zip	

1  
2  
3  
4  
5  
6  
7  
8  
9  
10  
11  
12  
13  
14  
15  
16  
17  
18  
19  
20  
21  
22  
23  
24  
25  
26  
27  
28  
29  
30  
31  
32  
33  
34  
35  
36  
37  
38  
39  
40  
41  
42  
43  
44  
45  
46  
47  
48  
49  
50  
51  
52  
53  
54  
55  
56  
57  
58  
59  
60



For Peer Review Only

1  
2  
3  
4  
5  
6 **Title:**  
7

8       **New prediction interval and band in the nonlinear regression model:**

9  
10 **Application to predictive modelling in foods**

11  
12  
13 **Authors:** Jean-Pierre Gauchi<sup>(1)\*</sup>, Jean-Pierre Vila<sup>(2)</sup>, Louis Coroller<sup>(3)</sup>  
14

15 **Affiliation:**

16  
17  
18       (1) INRA (National Institute of Agronomical Research)

19  
20  
21       Department of Applied Mathematics and Computational Science

22  
23       Unité MIA (UR341MIA); \*Corresponding author

24  
25  
26       Domaine de Vilvert, 78352 Jouy-en-Josas, France

27  
28       (2) INRA (National Institute of Agronomical Research)

29  
30  
31       Department of Applied Mathematics and Computational Science

32  
33       UMR Analyse des Systèmes et Biométrie

34  
35  
36       2, Place P. Viala, 34060 Montpellier, France

37  
38       (3) Université de Bretagne Occidentale, LUMAQ, Quimper, France

39  
40  
41 **E-mail of corresponding author:** Jean-Pierre.Gauchi@jouy.inra.fr

42  
43 **Postal address of corresponding author:**

44  
45       Dr. J.P. Gauchi / INRA / Unité MIA

46  
47       Domaine de Vilvert

48  
49  
50       78352 Jouy-en-Josas Cedex, France  
51  
52  
53  
54  
55  
56  
57  
58  
59  
60

1  
2  
3  
4  
5  
6 **Abstract:**  
7

8  
9 This paper is concerned with the proposal of a new **prediction interval** and  
10  
11 band for the nonlinear regression model. The construction principle of this interval  
12  
13 and band is based on an exact (the meaning of the term "exact" will be given  
14  
15 later) confidence region for parameters of the nonlinear regression model. This  
16  
17 region, fully described in Vila & Gauchi (2007), provides a rigorous justification  
18  
19 for the new **prediction interval** and band that we propose. This new band is  
20  
21 then compared to the classical bands (which are asymptotic and thus approximate  
22  
23 for small  $n$ ), and also to the band based on the bootstrap resampling method.  
24  
25 The comparison of these bands is undertaken with simulated and real data from  
26  
27 predictive modelling in food science.  
28  
29

30  
31 **Keywords:** **Prediction interval; Prediction band;** Nonlinear regression; Para-  
32  
33 metric confidence region; Predictive modelling; **Food Science.**  
34  
35  
36  
37  
38  
39  
40  
41

## 32 **1 Introduction**

33  
34 The question of the construction of **prediction intervals** ( $PI$ ) for a single value  
35  
36 or a mean and for **prediction bands** ( $PB$ ) was extensively studied and solved  
37  
38 in the case of linear regression models. The most frequently used solution was  
39  
40 developed by Working and Hotelling (1929) and is detailed in Draper and Smith  
41  
42 (1981). It leads to the familiar hyperbolic curves surrounding the regression model  
43  
44  
45  
46  
47  
48  
49  
50  
51  
52  
53  
54  
55  
56  
57  
58  
59  
60

1  
2  
3  
4  
5  
6 39 curve. However, several methods are always in competition for nonlinear regression  
7  
8  
9 40 models, and there is no rule for making a definitive choice for a given model. Our  
10  
11 41 aim is therefore to compare four well-known  $PI$  and  $PB$  on simulated and real data  
12  
13 42 to the new  $PI$  and  $PB$  we propose, using familiar predictive microbiology models  
14  
15  
16 43 in foods. The first two  $PI$  and  $PB$  are based on a first-order Taylor approximation  
17  
18 44 of the model analytic form and are called asymptotic  $PI$  and  $PB$  (see Bates and  
19  
20  
21 45 Watts, 1988). The third  $PI$  and  $PB$  are based on the bootstrap resampling method  
22  
23 46 (Efron and Tibshirani, 1993). The new  $PI$  and  $PB$  we propose are based on an  
24  
25  
26 47 exact (see Section 4 for the meaning of the term "exact") confidence parametric  
27  
28 48 region (the  $X$ -region fully described in Vila & Gauchi, 2007). The new  $PI$  will  
29  
30  
31 49 be referred to as  $PI_X$  and the new  $PB$  as  $PB_X$ .

32  
33 50 It is necessary to draw the reader's attention to a crucial point here. We are  
34  
35  
36 51 not actually dealing with genuine prediction regions (note the difference between  
37  
38 52 the words "regions" and "bands") of the model curve. A true prediction region  
39  
40  
41 53 for the model curve is a region where there is a fixed probability of finding this  
42  
43  
44 54 whole model curve completely inside this region. In fact, this question has not  
45  
46 55 yet been totally solved because a genuine region can be too large and of no use  
47  
48 56 to the practitioner. Thus, an approach based on a genuine prediction region is  
49  
50  
51 57 not always a relevant approach. Instead, we prefer to propose a  $PB$  made of joint  
52  
53 58 adjacent prediction intervals. The global predictive capability will therefore be  
54  
55  
56  
57  
58  
59  
60

1  
2  
3  
4  
5  
6 59 quantified by the band area. The rest of the article is organized as follows. Section  
7  
8 60 2 presents some useful notations for the reader. Section 3 provides information  
9  
10  
11 61 on asymptotic and bootstrap bands. Section 4 gives details on the new  $PI_X$  and  
12  
13 62  $PB_X$  we propose. Section 5 is devoted to the comparison of the four bands in the  
14  
15  
16 63 food science predictive modelling field; and Section 6 is the conclusion.

## 21 64 **2 Notations**

22  
23  
24  
25 65 Let us consider the standard parametric nonlinear regression model

$$26 \quad y_i = \eta(x_i, \theta^*) + \varepsilon_i \quad ; \quad i = 1, \dots, n \quad (1)$$

27  
28  
29  
30  
31  
32  
33 66 with the following notations: (a)  $y_i$  is the  $i^{\text{th}}$  observation of the response (the  
34  
35 67 corresponding  $n \times 1$  vector of the  $y_i$  is referred to as  $y$ ); (b)  $x_i$  is an  $m \times 1$  vector –  
36  
37 68 a support point – with component  $x_{il}$ ,  $l = 1, \dots, m$ , and  $x_i \in \Xi \subset \mathbb{R}^m$ , where  $\Xi$ ,  
38  
39 69 a compact subset of  $\mathbb{R}^m$ , is the experimental domain. For the sake of brevity, we  
40  
41  
42  
43 70 will refer to the  $n \times m$  matrix  $X$  as the whole set of the  $m$  explanatory variables set  
44  
45  
46 71 at  $n$  levels; (c) We assume that the errors  $\varepsilon_i$ , components of the  $n \times 1$  vector  $\varepsilon$ , are  
47  
48 72 independent and normally distributed; they have the same variance  $\sigma^2$  (generally  
49  
50  
51 73 unknown). Then,  $\varepsilon \sim \mathcal{N}(0, \Sigma)$ , where  $\Sigma = \sigma^2 I_n$  ( $I_n$  is the  $n \times n$  identity matrix); (d)  
52  
53 74  $\theta^*$  is the  $p \times 1$  vector of the unknown  $p$  parameters to be estimated,  $\theta^* \in \Theta \subset \mathbb{R}^p$ ,  
54  
55  
56 75 where  $\Theta$  is the parametric domain, a compact subset of  $\mathbb{R}^p$ ; (e)  $\eta(\cdot)$  is a continuous

1  
2  
3  
4  
5  
6 76 real-valued scalar function of  $x$  defined on  $\Xi \times \Theta$ , twice differentiable with respect  
7  
8  
9 77 to the parameters and the variables; we will simply refer to the corresponding  
10  
11 78  $n \times 1$  vector as  $\eta$  or  $\eta_\theta$  (function of the  $\theta$  variable); ( $f$ )  $n$  is the total number of  
12  
13 79 observations  $y_i$ .

14  
15  
16 80 We used the ordinary nonlinear least squares estimate  $\hat{\theta}$  as an estimate of  $\theta^*$

$$\hat{\theta} = \underset{\theta \in \Theta}{\text{Argmin}} \left\{ (y - \eta_\theta)^T \Sigma^{-1} (y - \eta_\theta) \right\} = \underset{\theta \in \Theta}{\text{Argmin}} \|y - \eta_\theta\|_\Sigma^2 \quad (2)$$

17  
18  
19  
20  
21  
22  
23  
24  
25 81 We also considered the Fisher information matrix  $M_F(X, \theta^*)$

$$M_F(X, \theta^*) = \sigma^{-2} J_{X, \theta^*}^T J_{X, \theta^*} \quad (3)$$

26  
27  
28  
29  
30  
31  
32  
33  
34 82 where  $J_{X, \theta^*}$  is the  $n \times p$  Jacobian matrix, with the  $j^{\text{th}}$  column consisting of the  $n$   
35  
36 83 components of  $\partial \eta(X, \theta^*) / \partial \theta_j^*$ ,  $j = 1, \dots, p$ .

37  
38  
39 84 A model prediction at any point  $x_i$  is defined as

$$\hat{y}_i = \eta(x_i, \hat{\theta}) \quad (4)$$

40  
41  
42  
43  
44  
45  
46  
47  
48 85 For further use, we also define the  $(1 \times p)$ -vector, a **row** of  $J_{X, \theta}$ , as:

$$\left[ \dot{\eta}(x_i, \hat{\theta}) \right]^T = \left( \frac{\partial \eta(x_i, \theta)}{\partial \theta_1} \Big|_{\theta_1 = \hat{\theta}_1} \cdots \frac{\partial \eta(x_i, \theta)}{\partial \theta_p} \Big|_{\theta_p = \hat{\theta}_p} \right). \quad (5)$$

### 3 Classical *PI* and *PB*

#### 3.1 Principle

As reported by Khorasani & Milliken (1982), the problem of constructing a prediction band around a regression model can be viewed as a problem of simultaneously constructing an infinite set of confidence intervals. Let us assume that  $E(y_0) = \eta(x_0, \theta^*)$  is the mean of some  $y_0$ , and that  $\hat{y}_0 = \hat{E}(y_0) = \eta(x_0, \hat{\theta})$ , the mean prediction, is its estimation. We are interested in determining a *PI* for  $y_0$ , followed by a *PB* for the regression model. The objective will be fully satisfied if the confidence level of the *PIs* and that of the *PBs* is as close as possible to  $1 - \alpha$  where  $\alpha$  is a **first-kind error**.

Thus, the first step is to construct a *PI* for  $y_0$  (located on  $x_0$ ) defined as:

$$PI(y_0, x_0, \alpha) = [L(\hat{y}_0, x_0, \alpha) ; U(\hat{y}_0, x_0, \alpha)]$$

where  $L(\hat{y}_0, x_0, \alpha)$  is the lower bound of the interval, and  $U(\hat{y}_0, x_0, \alpha)$  is the upper bound of the interval.

The second step is then to determine a *PB* over  $\Xi$ . It should be observed that if  $\Xi \subset R^m$ , with  $m = 1$ , we then consider a band, but if  $m \geq 2$ , we will refer to it as a **prediction region** (*PR*), different from a genuine prediction region (see the crucial point in the introduction). The upper curve (or the  $m$ -dimensional

1  
2  
3  
4  
5  
6 upper surface) of the **prediction band** (or a *PR*) is theoretically made up of  
7  
8  
9 an infinite number of upper ends (points) of adjacent *PI*, and the lower curve  
10  
11 is made in a similar way. From a practical point of view, a large number  $K$  of  
12  
13 adjacent *PI* at  $K$  support points  $x_i$  will be built. Typically,  $K$  is equal to 200  
14  
15 when  $m = 1$ , and  $K \geq 1000$  when  $m > 1$ . It should be observed that if  $m$  is large  
16  
17 – typically larger than 4 – then a Monte Carlo approach would be necessary for  
18  
19 randomly (uniformly) choosing the locations  $x_i$  in  $\Xi$  where  $U(\cdot)$  and  $L(\cdot)$  could be  
20  
21 computed. Alternatively, other methods such as grid methods could be used. For  
22  
23 characterizing a band (or a region), we propose to determine an approximation  
24  
25 of its area  $\mathcal{A}$  (or its volume  $\mathcal{V}$ ) by means of a standard numerical integration (a  
26  
27 procedure based on the summation of elementary rectangles that form the band,  
28  
29 or a usual Monte Carlo integration procedure in the case of a region).  
30  
31  
32  
33  
34  
35  
36  
37

### 114 3.2 Intervals and bands based on an asymptotic approach

115 Let us consider the random variable

$$\hat{T} = \frac{\hat{y}_0 - y_0}{h_{x_0}^{1/2}(\hat{\theta})} \quad (6)$$

116 where

$$h_{x_0}(\hat{\theta}) = \hat{\sigma}^2 \left[ \dot{\eta}(x_0, \hat{\theta}) \right]^T \left( J_{X, \hat{\theta}}^T J_{X, \hat{\theta}} \right)^{-1} \left[ \dot{\eta}(x_0, \hat{\theta}) \right] \quad (7)$$

1  
2  
3  
4  
5  
6 and where

$$\hat{\sigma}^2 = \frac{1}{n-p} \sum_{i=1}^n (y_i - \hat{y}_i)^2 \quad (8)$$

7  
8  
9  
10  
11  
12  
13  
14 Classical asymptotic theory (Gallant, 1987) tells us that the limiting distribution  
15  
16 (when  $n$  tends to infinity) of (6) is a centered normal distribution  $\mathcal{N}(0, 1)$  where  
17  
18  
19  
20  
21  
22  
23  
24  
25  
26  
27  
28  
29  
30  
31  
32  
33  
34  
35  
36  
37  
38  
39  
40  
41  
42  
43  
44  
45  
46  
47  
48  
49  
50  
51  
52  
53  
54  
55  
56  
57  
58  
59  
60  
120  $h_{x_0}^{1/2}(\hat{\theta})$  is an estimate of the standard error of  $\hat{y}_0$ . However, for small fixed  $n$ ,  
121 the true distribution of  $\hat{T}$  is not a normal one and is not known. Nevertheless,  
122 we have somewhat accurate approximations of the true distribution when  $n$  is not  
123 infinite, which lead to confidence interval approximations. Typically, on the basis  
124 of Gallant (1987), we have:

$$PI_t(y_0, x_0, \alpha) = [\hat{y}_0 - t_{n-p;1-\alpha/2} h_{x_0}^{1/2}; \hat{y}_0 + t_{n-p;1-\alpha/2} h_{x_0}^{1/2}] \quad (9)$$

125 where  $t_{n-p;1-\alpha/2}$  is the  $(1-\alpha/2)$ -percentile for the Student distribution with  $n-p$   
126 degrees of freedom. The whole set of the joint  $PI_t$ s leads to the  $PB_t$ .

127 On the basis of Bates & Watts (1988), we can use a good alternative defined as:

$$PI_F(y_0, x_0, \alpha) = \left[ \hat{y}_0 - (h_{x_0} p \mathcal{F}_{p, n-p; \alpha})^{1/2}; \hat{y}_0 + (h_{x_0} p \mathcal{F}_{p, n-p; \alpha})^{1/2} \right] \quad (10)$$

128 where  $\mathcal{F}_{p, n-p; \alpha}$  is the upper  $\alpha$ -percentile for the **Fisher-Snedecor** distribution  
129 with  $p$  and  $n-p$  degrees of freedom. This interval definition leads to a so-called

1  
2  
3  
4  
5  
6 130 simultaneous **prediction band**  $PB_F$ .

7  
8  
9 131 These methods are called asymptotic in the nonlinear case because it has been  
10  
11 132 proven (see Gallant, 1987) that  $PI_t$  and  $PI_F$  tend to an exact  $PI$  as  $n \rightarrow \infty$ . In  
12  
13 133 this case, the word "exact" means that the coverage probability of  $y_0$  is exactly  
14  
15 134 equal to  $1 - \alpha$ . For a fixed  $n$ , particularly if  $n$  is small,  $PI_t$  and  $PI_F$  are only  
16  
17 135 approximate, and their covering probabilities are not equal to  $1 - \alpha$ , and are close  
18  
19 136 to  $1 - \alpha$  if  $n$  is large enough.  
20  
21  
22  
23  
24

### 25 137 **3.3 Interval and band based on the bootstrap method**

26  
27  
28 138 This method is based on the famous resampling method called the bootstrap  
29  
30 139 method (Efron and Tibshirani, 1993). Many statistics can be estimated with this  
31  
32 140 method, particularly the construction of confidence intervals, as clearly described  
33  
34 141 in Huet et al. (2004, page 138). We only give the results here:  
35  
36  
37  
38  
39

$$40 \quad PI_B(y_0, x_0, \alpha) = \left[ \hat{y}_0 - b_{1-\alpha/2} h_{x_0}^{1/2}(\hat{\theta}) ; \hat{y}_0 - b_{\alpha/2} h_{x_0}^{1/2}(\hat{\theta}) \right] \quad (11)$$

41  
42  
43  
44 142 where  $b_{1-\alpha/2}$  and  $b_{\alpha/2}$  are the  $1 - \alpha/2$ -percentile and  $\alpha/2$ -percentile, respectively,  
45  
46 143 of the bootstrap distribution of  $\hat{y}_0$ . Generally, for a given  $n$  (not infinity), it can  
47  
48 144 be assumed that  $PB_B$  will be narrower than  $PB_t$  and  $PB_F$  for a confidence level  
49  
50 145 close to  $1 - \alpha$ .  
51  
52  
53  
54  
55  
56  
57  
58  
59  
60

## 146 4 A new prediction band

### 147 4.1 The $X$ -region

148 Because the  $PB_X$  is based on an exact confidence region for the parameters of a  
 149 nonlinear regression model – the  $X$ -region fully described in Vila and Gauchi  
 150 (2007) – we have included the following definition for the reader's information:

151 **Definition 1** *Let  $C(\theta^*)$  be the covering probability of  $\theta^*$ . The confidence region of*  
 152 *nominal level  $\alpha$  for  $\theta^*$  is then said to be approximate if  $C(\theta^*) \approx 1 - \alpha$ , asymptotic*  
 153 *if  $\lim_{n \rightarrow \infty} C(\theta^*) = 1 - \alpha$ , conservative if  $C(\theta^*) \geq 1 - \alpha$ , and exact if  $C(\theta^*) = 1 - \alpha$ ,*  
 154  *$\forall n$ .*

155 The  $X$ -region we used is defined as:

$$37 \quad \mathfrak{R}_X(\theta^*, y) = \{\theta \in \Theta : R_X(\theta) \leq \mathcal{F}_{p,\nu;\alpha}\} \quad (12)$$

156 where  $R_X(\theta) = (y - \eta_\theta)^T P_\theta (y - \eta_\theta) / ps_\nu^2$  with  $P_\theta = J_{X,\theta} (J_{X,\theta}^T J_{X,\theta})^{-1} J_{X,\theta}^T$ , the usual  
 157 projector onto the plane, tangent at  $\eta_\theta$ , on the model response surface (see Bates  
 158 and Watts, 1988, p.36, for a clear presentation), and  $s_\nu^2$  an estimate of  $\sigma^2$ , based  
 159 on  $\nu$  degrees of freedom (d.o.f.).  $\mathcal{F}_{p,\nu;\alpha}$  is the  $\alpha$ -percentile of the Fisher-Snedecor  
 160 distribution  $\mathcal{F}_{p,\nu}$  with  $p$  and  $\nu$  d.o.f. If  $s_\nu^2$  is not available, it will be replaced by the  
 161 mean square error (and, thus,  $\nu = n - p$  in this case) of the regression procedure.  
 162 A graph of this region is displayed in Vila and Gauchi (2007). It may look very

1  
2  
3  
4  
5  
6 163 different from the ellipsoidal confidence region often used as an approximative  
7  
8  
9 164 region.

10  
11 165 We would like to remind the reader here of some important properties of the  
12  
13 166  $X$ -region (Vila and Gauchi, 2007): the  $X$ -region does not depend on intrinsic  
14  
15  
16 167 and parametric nonlinearities of the model  $\eta(\cdot)$ , and the true  $\Theta$  is taken into  
17  
18 168 account in its construction. These properties are enhanced if  $n$  is small and  $\sigma$  is  
19  
20  
21 169 large. Consequently, the  $PB_X$  will benefit from these properties of the  $X$ -region,  
22  
23 170 to the contrary of the preceding  $PBs$ . Indeed, we know that these two conditions  
24  
25  
26 171 make the usual first-order approximation involved in  $PI_t$  and  $PI_F$  inadequate.

## 172 4.2 The $PB_X$

173 We can now construct the  $PB_X$ . This band is formed by joining  $K$  (see Subsection  
174 3.1) adjacent  $PI_X$ . A  $PI_X$  for  $y_i$  is then built by means of the four steps of the  
175 following simple algorithm based on Monte Carlo samplings:

### 176 Step 1

177 If  $p \leq 3$ : uniformly sample a large number  $Q$  of vectors  $\tilde{\theta}_u \in \Theta$ ,  $u = 1, \dots, Q$   
178 (typically  $Q = 1000$  for  $p = 1$ ,  $Q = 10^4$  for  $p = 2$ ,  $Q = 5 \times 10^4$  for  $p = 3$ , since  
179 these values are now easily attainable with powerful modern computers).  
180 Among the  $Q$  vectors  $\tilde{\theta}_u$ , only  $Q^*$  satisfy the inequality in (12). Thus, the  
181 set of these  $Q^*$  vectors  $\tilde{\theta}_u$  forms an approximation of the volume of (12).

1  
2  
3  
4  
5  
6 182 If  $p > 3$ : sample a large number  $Q$  of uniform random straight half lines  $L_k \in \Theta$ ,  
7  
8  
9 183  $k = 1, \dots, Q$ , whose origins are all located at  $\theta_0$  and whose slopes are random  
10  
11 184 (typically  $Q = 10^4$  for  $p = 4, 5$ , or  $6$ ,  $Q = 10^5$  for  $6 < p \leq 10$ ). On each  
12  
13 185 random line  $L_k$ , choose a number  $q_k$  of values  $\tilde{\theta}_u$ ,  $u = 1, \dots, q_k$ , regularly  
14  
15  
16 186 spaced on this line. The same stepsize is used for all the lines, and each  $q_k$   
17  
18 187 depends on the proximity of  $\theta_0$  from the border of the  $X$ -region along the  
19  
20  
21 188  $L_k$  line. Finally, only  $Q^*$  vectors  $\tilde{\theta}_u$  among the  $\sum_{k=1}^Q q_k$  vectors satisfy the  
22  
23 189 inequality in (12). It should be observed that the sampling used for  $p \leq 3$   
24  
25  
26 190 would be very ineffective here because it is well-known that the random  $\tilde{\theta}_u$   
27  
28 191 would be increasingly often located in the corners of  $\Theta$  when the dimension  
29  
30  
31 192 of  $\Theta$  increases.

32  
33  
34 193 **Step 2** Choose  $x_i$  as the place in  $\Xi$  where we want to make a prediction.

35  
36  
37 194 **Step 3** Compute the  $Q^*$  values  $\hat{y}_i^{(u)} = \eta(x_i, \tilde{\theta}_u)$ ,  $u = 1, \dots, Q^*$ .

38  
39  
40 195 **Step 4** Determine the lower bound of the  $PI_X$  by  $L = \min_u \{\hat{y}_i^{(u)}\}$ , and the upper  
41  
42  
43 196 bound of the  $PI_X$  by  $U = \max_u \{\hat{y}_i^{(u)}\}$ .

44  
45  
46  
47 197 The exact confidence level of this band is not yet clear but we can assume that it  
48  
49 198 tends to  $\beta \geq 1 - \alpha$  when  $Q^*$  increases because the function  $\eta(x_i, \theta)$  is surjective  
50  
51  
52 199 relative to  $\theta$ . Consequently, the  $PB_X$  is a conservative band.

1  
2  
3  
4  
5  
6 200 **5 Applications to predictive modelling in food**  
7  
8  
9  
10 201 **science**

11  
12  
13  
14 202 **5.1 A primary growth model: the Baranyi & Roberts model**

15  
16  
17 203 **5.1.1 Definition**

18  
19  
20 204 The analytic form of this model (the deterministic part) proposed by Baranyi and  
21  
22  
23 205 Roberts (1994, 1995), including four parameters and one explanatory factor, is:

$$\eta(\theta^*, t) = \frac{1}{\ln(10)} [\ln(x_0) + \mu_{\max} A(\theta^*, t) - \ln(B(\theta^*, t))]$$

24  
25  
26  
27  
28  
29  
30  
31  
32  
33  
34  
35  
36 206 where

$$A = t + \frac{1}{\mu_{\max}} \ln(A_0)$$

$$A_0 = \exp(-\mu_{\max} t) + \exp(-\mu_{\max} lag) - \exp(-\mu_{\max} t - \mu_{\max} lag)$$

$$B = 1 + \frac{[\exp(\mu_{\max} A)] - 1}{\frac{x_{\max}}{x_0}}$$

37  
38  
39  
40  
41  
42  
43  
44  
45  
46  
47  
48  
49  
50  
51 207 with  $\mu_{\max}$  (maximum growth rate),  $lag$  (lag time before growth, in hours),  $x_{\max}$   
52  
53  
54 208 (maximal number of bacteria),  $x_0$  (initial number of bacteria), the four components

of  $\theta^*$ , and time  $t$  (the explanatory factor).  $\eta(\theta^*, t)$  is the number of bacteria (in log units).

### 5.1.2 Results with simulated data

We first present an illustration with the *a priori* values  $\mu_{\max 0} = 1$ ;  $lag_0 = 5$ ;  $x_{\max 0} = 10^8$ ;  $x_{00} = 100$ , and  $\Theta = [0.5; 1.5]_{\mu_{\max 0}} \times [2; 8]_{lag_0} \times [0.5 \times 10^8; 1.5 \times 10^8]_{x_{\max 0}} \times [50; 150]_{x_{00}}$ , and  $\Xi = [0, 50]$ . With this information (from the SYMPREVIUS Research Group, see Acknowledgements Section) we simulated ten Gaussian  $y_i$  values (with standard deviation equal to 0.1) at ten equidistant levels of time. We obtained Fig. 1 after computation of  $\hat{\theta} = (1.18 ; 5.44 ; 1.5 \times 10^8 ; 50)^T$  by means of the NLIN procedure of SAS/STAT software.

*The figure 1 should be approximately placed here*

Fig. 1: The four bands for the Baranyi-Roberts model for one **simulated** data set (crosses stand for the simulated data). The values of the band areas (calculated with procedures indicated at the end of Subsection 3.1) are:  $\mathcal{A}(PB_t) = 21$ ;  $\mathcal{A}(PB_F) = 36$ ;  $\mathcal{A}(PB_B) = 24$ ;  $\mathcal{A}(PB_X) = 42$ .

For a more relevant comparison, we simulated 1000 data sets, each data set being defined as the pairs  $\{(t_u, \tilde{y}_u) ; u = 1, \dots, 10\}$ , where the  $t_u$  were always equal to the ten previous levels. Each random  $\tilde{y}_u$  was generated by a Gaussian distribution

227  $\mathcal{N}(y_i, \sigma_S)$  where  $y_i$  was the previous simulated value. Three values of  $\sigma_S$  were used:  
 228  $\sigma_S = 0.05; 0.1; 0.5$ , these values being typical of real experimental situations. For  
 229 each  $\sigma_S$ -situation, we provide the simulation results in Table 1.

Areas	min	max	mean	std	cv%
$\mathcal{A}(PB_t)$	33 ; 31 ; 38	40 ; 44 ; 91	36 ; 37 ; 63	1.5 ; 3 ; 12	4 ; 8 ; 20
$\mathcal{A}(PB_F)$	57 ; 54 ; 66	69 ; 77 ; 159	63 ; 65 ; 110	2.6 ; 5 ; 21	4 ; 8 ; 19
$\mathcal{A}(PB_B)$	60 ; 60 ; 82	86 ; 125 ; 252	78 ; 97 ; 191	6 ; 18 ; 44	7 ; 18 ; 8
$\mathcal{A}(PB_X)$	62 ; 61 ; 46	64 ; 66 ; 71	63 ; 63 ; 61	0.6 ; 1 ; 5	1 ; 1.7 ; 8

231 Table 1: Baranyi-Roberts model: Simulation statistics of the band areas based on  
 232 1000 simulated data sets. The figures are given sequentially according to  $\sigma_S = 0.05;$   
 233  $0.1; 0.5$ , respectively. For example, for  $\sigma_S = 0.05$ , we obtain  $\min(\mathcal{A}(PB_t)) = 33,$   
 234  $\max(\mathcal{A}(PB_t)) = 40,$   $\text{mean}(\mathcal{A}(PB_t)) = 36,$   $\text{std}(\mathcal{A}(PB_t)) = 1.5,$   $\text{cv}\%(\mathcal{A}(PB_t)) =$   
 235 4.

### 236 5.1.3 An illustration with real data

237 With real data (obtained from the SYMPREVIUS Research Group, see Acknowl-  
 238 edgements Section) we obtained Fig. 2 where the estimated model curve is based  
 239 on  $\hat{\mu}_{\max} = 0.055; \widehat{\text{lag}} = 42; \hat{x}_{\max} = 1.52 \times 10^8; \hat{x}_0 = 4005; \Theta = [0.050; 0.060]_{\mu_{\max}0}$   
 240  $\times [30; 54]_{\text{lag}0} \times [38124759; 266660000]_{x_{\max}0} \times [2715; 5294]_{x_{00}},$  and  $\Xi = [0; 310].$

241 *The figure 2 should be approximately placed here*

1  
2  
3  
4  
5  
6 242 Fig. 2: The four bands for the Baranyi-Roberts model for one real data set  
7  
8  
9 243 (crosses stand for the real data). The values of the band areas are:  $\mathcal{A}(PB_t) = 70$ ;  
10  
11 244  $\mathcal{A}(PB_F) = 111$ ;  $\mathcal{A}(PB_B) = 98$ ;  $\mathcal{A}(PB_X) = 166$ .  
12  
13  
14  
15  
16  
17  
18  
19  
20  
21  
22

#### 246 5.1.4 Discussion

247 We can see on Fig. 1 that the  $PB_t$  and  $PB_F$  bands are totally inadequate when  
248 the model appears as a zero-slope straight line. Indeed, the band is reduced to a  
249 single line while the variability of the prediction is not null. On the contrary, the  
250 other two bands seem more realistic since their width is not null. Moreover, we  
251 can see on Fig. 2 that more data lie outside the  $PB_t$ ,  $PB_F$  and  $PB_B$ , contrast  
252 to the  $PB_X$ . In Table 1, we can observe that the  $PB_X$  does not appear to be not  
253 very sensitive to the change of the simulation  $\sigma_S$ ; moreover, its area is close to  
254 that of the  $PB_F$ .  
25  
26  
27  
28  
29  
30  
31  
32  
33  
34  
35  
36  
37  
38  
39  
40  
41  
42  
43  
44  
45  
46  
47  
48  
49  
50  
51  
52  
53  
54  
55  
56  
57  
58  
59  
60

## 255 5.2 An inactivation model: the double-Weibull model

### 256 5.2.1 Definition

The analytic form of this model (the deterministic part) proposed by Coroller (2006), including five parameters and one explanatory factor, is:

$$\eta(\theta^*, t) = C - \log_{10}(1 + 10^\alpha) + \log_{10} \left[ 10^{-\left(\frac{t}{\delta_1}\right)^p + \alpha} + 10^{-\left(\frac{t}{\delta_2}\right)^p} \right]$$

257 where  $C = \log_{10} N_0$  (where  $N_0$  is the initial number of bacteria),  $\alpha$  and  $p$  are shape  
 258 parameters,  $\delta_1$  and  $\delta_2$  are treatment times for the first decimal reductions,  $\eta(\theta^*, t)$   
 259 is the bacteria number (in log units), and  $t$  is the time (in hours), the explanatory  
 260 factor. The vectorial parameter we are interested in is  $\theta = (C, \alpha, p, \delta_1, \delta_2)^T$ .

### 261 5.2.2 Results with simulated data

262 We first present an illustration with the *a priori* values  $C_0 = 5.45$ ;  $\alpha_0 = 3.15$ ;  
 263  $p_0 = 3.67$ ;  $\delta_{10} = 5.45$ ;  $\delta_{20} = 17.21$ , and  $\Theta = [5; 6]_{C_0} \times [2; 4]_{\alpha_0} \times [1.5; 6]_{p_0} \times$   
 264  $[4; 7]_{\delta_{20}} \times [12; 20]_{\delta_{20}}$ , and  $\Xi = [0; 20]$  (Coroller, 2006). Using this information  
 265 we simulated 20 Gaussian  $y_i$  values (with standard deviation equal to 0.1) at  
 266 20 equidistant levels of time. We obtained Fig. 3 after computation of  $\hat{\theta} =$   
 267  $(5.56 ; 3.15 ; 2.99 ; 5.17 ; 16.50)^T$  by means of the NLIN procedure of SAS/STAT  
 268 software.

269 *The figure 3 should be approximately placed here*

270 Fig. 3. The four bands for the **Coroller** model for one **simulated** data set (crosses  
 271 stand for the simulated data). The values of the band areas are:  $\mathcal{A}(PB_t) = 7.82$ ;  
 272  $\mathcal{A}(PB_F) = 13.97$ ;  $\mathcal{A}(PB_B) = 8.90$ ;  $\mathcal{A}(PB_X) = 13.38$ . It should be noted that  
 273 days appear on the abscisses, but the parameters are given in the text for the time  
 274 in hours.

275  
 276 For a more relevant comparison, we simulated 1000 data sets, each data set being  
 277 defined as the pairs  $\{(t_u, \tilde{y}_u); u = 1, \dots, 10\}$  where  $t_u$  were always equal to the  
 278 20 previous levels. We proceeded as in Subsection 5.1.2, and we obtained the  
 279 simulation results given in Table 2.

Areas	min	max	mean	std	cv%
$\mathcal{A}(PB_t)$	8 ; 8 ; 19	10 ; 13 ; 35	9 ; 10 ; 26	0.5 ; 0.96 ; 3.7	5 ; 9 ; 14
$\mathcal{A}(PB_F)$	15 ; 15 ; 33	19 ; 22 ; 62	17 ; 19 ; 47	0.89 ; 1.7 ; 6.6	5 ; 9 ; 14
$\mathcal{A}(PB_B)$	10 ; 11 ; 29	26 ; 42 ; 96	20 ; 32 ; 73	4 ; 8 ; 13	20 ; 24 ; 18
$\mathcal{A}(PB_X)$	31 ; 31 ; 36	33 ; 33 ; 35	32 ; 32 ; 31	0.36 ; 0.54 ; 1.95	1.1 ; 1.7 ; 6

281 Table 2 : Coroller model: Simulation statistics of the band areas. The figures are  
 282 given sequentially according to  $\sigma_S = 0.05; 0.1; 0.5$ , respectively. The figures have  
 283 been rounded off.

### 284 5.2.3 An illustration with real data

285 With real data (Coroller, 2006), we obtained Fig. 4 where the estimated model  
286 curve is based on  $\hat{C}_0 = 5.39$ ;  $\hat{\alpha} = 3.06$ ;  $\hat{\rho} = 3.53$ ;  $\hat{\delta}_1 = 5.54$ ;  $\hat{\delta}_2 = 17.44$ .

287 *The figure 4 should be approximately placed here*

288 Fig. 4: The four bands for the Coroller model for one real data set (crosses  
289 stand for the real data). The values of the band areas are:  $\mathcal{A}(PB_t) = 9$ ;  $\mathcal{A}(PB_F) =$   
290  $15.78$ ;  $\mathcal{A}(PB_B) = 9.33$ ;  $\mathcal{A}(PB_X) = 16.54$ .

### 291 5.2.4 Discussion

292 This real application is particularly relevant for demonstrating the usefulness of  
293 the  $PB_X$ . Indeed, a crucial point here is to have a realistic PCI at the place where  
294 the model begins to break down (after about eight days in Fig. 4). At that time,  
295 the microbiologist needs a realistic PCI for the log number of bacteria present in  
296 the experiment. In this case, we can observe that  $PI_t$  and  $PI_B$  are completely  
297 false. We confirm that the  $PB_X$  is not very sensitive to the simulation  $\sigma_S$ . Its  
298 area is slightly larger than that of other bands, but that does not prevent its future  
299 use.

### 300 5.3 Another inactivation model: the Leguerinel et al. model

#### 301 5.3.1 Definition

302 The analytic form of this model (the deterministic part) proposed by Leguerinel  
 303 et al. (2005) for modelling the logarithm of the decreasing number of bacteria,  
 304 including five parameters and three explanatory factors, is:

$$\eta(\theta; t, pH, Aw) = 5 - \left( \frac{t}{\delta \times 10 \left[ \left( \frac{pH - pH_{opt}}{Z_{pH}} \right)^2 + \left( \frac{Aw - 0.985}{Z_{Aw}} \right)^2 \right]} \right)^p$$

305 where the vector parameter is  $\theta = (p, \delta, Z_{pH}, Z_{Aw}, pH_{opt})^T$ , and the explanatory  
 306 factors are  $t$  (the time in minutes),  $pH$ , and water activity  $Aw$ . Because no  
 307 rigorous design has yet to be found, real data are not available at that moment  
 308 for the modelling of such a model. However, it is of particular importance to run  
 309 some simulations for comparing the different regions. The *a priori* values provided  
 310 by Leguérinel et al. (2005) for the parameters and domains are:

$$p_0 = 5; \delta_0 = 1.8; Z_{pH0} = 2.18; Z_{Aw0} = 0.092; pH_{opt0} = 6.96$$

$$\Theta_0 = [4.5; 5.5]_{p_0} \times [1.6; 2]_{\delta_0} \times [2; 2.5]_{Z_{pH0}} \times [0.0917; 0.0930]_{Z_{Aw0}} \times [6.5; 7.2]_{pH_{opt0}}$$

$$\Xi = [0; 5378]_t \times [4; 9]_{pH} \times [0.9; 1]_{Aw}$$

1  
2  
3  
4  
5  
6 311 The 72 simulated values were obtained by forming a 3-dimensional grid on  $\Xi$ ,  
7  
8 312 with respect for the constraint  $\eta(\cdot) \geq 1$  throughout. Table 3 gives the results  
9  
10  
11 313 based on 100 simulated data sets, obtained with  $\sigma_S = 0.2$ .

Volumes	min	max	mean	std	cv%
$\mathcal{V}(PR_t)$	2.68	2.95	2.82	0.06	2.15
$\mathcal{V}(PR_F)$	4.55	5.01	4.79	0.10	2.14
$\mathcal{V}(PR_X)$	36.50	38.20	37.26	0.74	2.02

12  
13  
14  
15  
16  
17 314  
18  
19  
20  
21  
22  
23  
24 315 Table 3: Inactivation model: simulation statistics of the band areas for  $\sigma_S = 0.2$ .  
25  
26 316  $\mathcal{V}(PR_B)$  do not appear here because they are too time-consuming (one compu-  
27  
28 317 tation of  $\mathcal{V}(PR_B)$  alone requires about ten hours, while  $\mathcal{V}(PR_t)$  and  $\mathcal{V}(PR_F)$   
29  
30 318 require less than three minutes, and  $\mathcal{V}(PR_X)$  require about one hour; all the com-  
31  
32 319 putations were carried out under the same conditions on a Pentium IV Personal  
33  
34  
35  
36 320 Computer).

### 321 5.3.2 Discussion

322 This model leads to a larger volume for  $PR_X$  but, as in the preceding examples,  
323 this **region** is usable mainly because it is a conservative **region**.

## 6 Conclusion

We now have a relevant and a statistically rigorous  $PB$  – the  $PB_X$  – for evaluating the global predictive capability of a nonlinear regression model. Since we were able to observe in the preceding examples that its area is not too large, on the one hand, and keeping in mind that it is a conservative band, on the other hand, we are convinced that the  $PB_X$  can become a useful tool for the practitioner in predictive modelling in food. The two usual bands,  $PB_t$  and  $PB_F$ , **can lead to a weak accuracy and, consequently, can be incorrect**, especially when  $n$  and  $\sigma^2$  are large. The  $PB_B$  is based on a second-order approximation, not an exact basis.

The algorithm proposed in Subsection 4.2 for determining the  $PB_X$  is easy to code and quick to run. Even with five parameters and three explanatory factors in the model (example of Subsection 5.3), less than one hour is necessary on a Pentium IV Personal Computer. The  $PB_B$  is too time-consuming, even for  $p = 3$ .

The  $PB_X$  could be effectively used for the comparison of two models by considering the eventual overlapping of their bands. If the two bands overlap, then we will assume that these two models are not significantly different for fitting the data collected, and different if no overlapping exists at all. The intermediate case where overlapping is partial obviously remains a difficult case to resolve. More research is needed in this situation. Finally, a complementary study must be carried out

1  
2  
3  
4  
5  
6 344 when the variance is heteroscedastic. This work is in progress.  
7  
8

9       **Acknowledgements:** We would like to express our gratitude to the following  
10 345  
11 institutions, members of the SYMPREVIUS Research Group: ADRIA-Quimper,  
12 346  
13 LUMAQ, INRA, Soredab, CTSCCV, ENVA, AERIAL, for providing data and  
14 347  
15 submitting this problem of **prediction bands** in predictive modelling in foods.  
16 348  
17  
18  
19  
20  
21

## 22 349 **7 References**

- 23  
24  
25 350 Baranyi, J., Pin, C., Ross, T. (1999). Validating and comparing predictive models.  
26  
27 International Journal of Food Microbiology 48: 159-166.  
28 351  
29  
30 352 Baranyi, J., Roberts, T.A. (1994). A dynamic approach to predicting bacterial  
31  
32 growth in food. International Journal of Food Microbiology 23: 277-294.  
33 353  
34  
35 354 Baranyi, J., Roberts, T.A. (1995). Mathematics of predictive food microbiology.  
36  
37 International Journal of Food Microbiology 26: 199-218.  
38 355  
39  
40 356 Bates, D.M., Watts, D.G. (1988). *Nonlinear regression analysis and its applica-*  
41  
42 *tions*. John Wiley & Sons, New York.  
43 357  
44  
45 358 Coroller, L. (2006). General model based on two mixed Weibull distributions of  
46  
47 bacterial resistance for describing various shapes of inactivation curves. Applied  
48 359  
49 and Environmental Microbiology 72: 10, 6493-6502.  
50 360  
51  
52 361 Draper, N.R., Smith, H. (1981). *Applied regression analysis*. Second Edition.  
53  
54 Wiley, New-York.  
55 362  
56  
57  
58  
59  
60

- 1  
2  
3  
4  
5  
6 363 Efron, B., Tibshirani, R.J. (1993). *An introduction to the bootstrap*. Chapman &  
7  
8 364 Hall.  
9  
10  
11 365 Gallant, A.R. (1987). *Nonlinear statistical models*. Wiley & sons.  
12  
13  
14 366 Huet, S., Bouvier, A., Poursat, M.-A., Jolivet E. (2004). *Statistical Tools for*  
15  
16 367 *Nonlinear Regression. A Practical Guide with S-PLUS and R Examples*. Second  
17  
18 368 Edition. Springer Series in Statistics  
19  
20  
21 369 Khorasani, F., Milliken, G.A. (1982). Simultaneous confidence bands for nonlinear  
22  
23 370 regression models. *Commun. Statist.-Theor. Meth.* 11: 11, 1241-1253.  
24  
25  
26 371 Leguérinel, I., Spegagne, I., Couvert, O., Gaillard, S., Mafart, P. (2005). Val-  
27  
28 372 idation of an overall model describing the effect of three environmental factors  
29  
30 373 on the apparent D-value of *Bacillus cereus* spores. *International Journal of Food*  
31  
32 374 *Microbiology* 100: 1-3, 223-229.  
33  
34  
35 375 Oscar, T.P. (2005). Validation of Lag Time and Growth Rate Models for *Salmonella*  
36  
37 376 *Typhimurium*: Acceptable Prediction Zone Method. *Journal of Food Science* 70:  
38  
39 377 129-137.  
40  
41  
42  
43 378 Ross, T. (1996). Indices for performance evaluation of predictive. References  
44  
45 379 models in food microbiology. *Journal of Applied Bacteriology* 81: 501-508.  
46  
47  
48 380 SAS/IML and SAS/STAT Software, Version 8.1. SAS Institute. Cary. North  
49  
50  
51 381 Carolina. USA.  
52  
53 382 Vila, J.-P., Gauchi, J.-P. (2007). Optimal designs based on exact confidence regions  
54  
55  
56  
57  
58  
59  
60

1  
2  
3  
4  
5  
6 383 for parameter estimation of a nonlinear regression model. J. of Statistical Planning  
7  
8  
9 384 and Inference 137: 9, 2935-2953.

10  
11 385 Working, H., Hotelling, H. (1929). Applications of the theory of error to the  
12  
13  
14 386 interpretation of trends. Journal of the American Statistical Association 24: 73-  
15  
16 387 85.

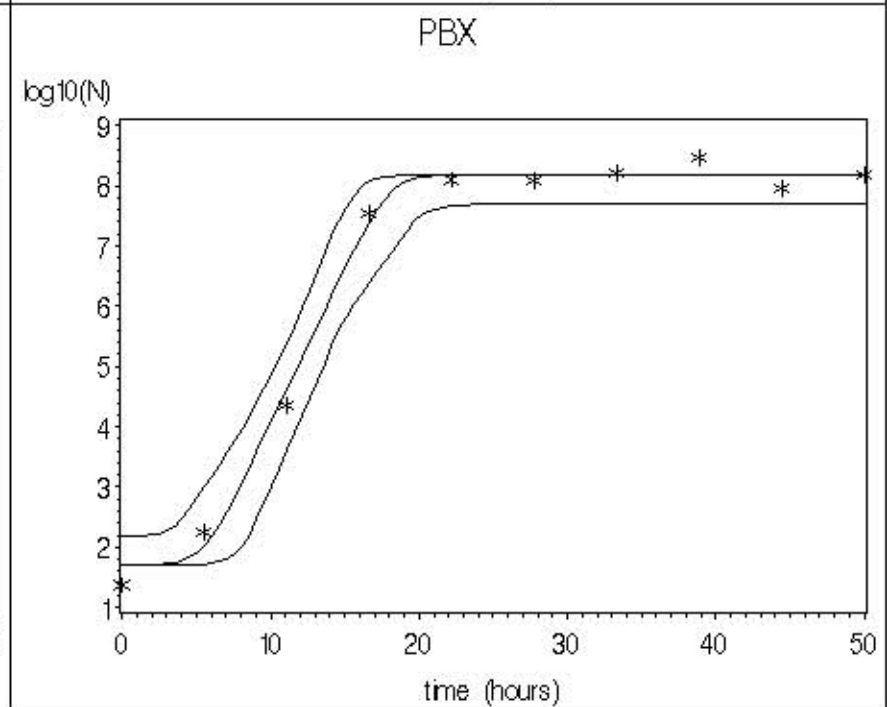
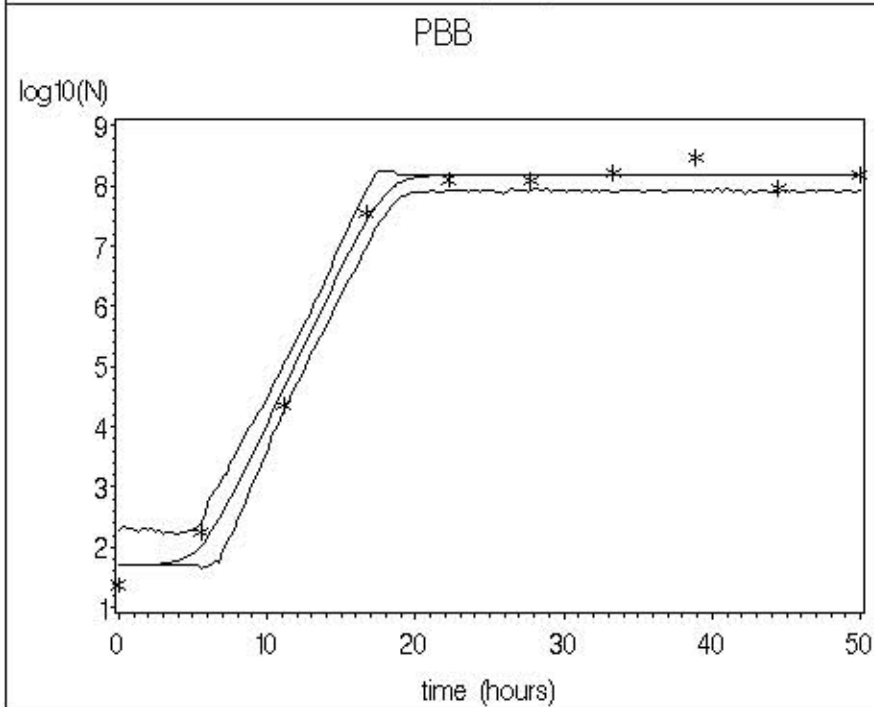
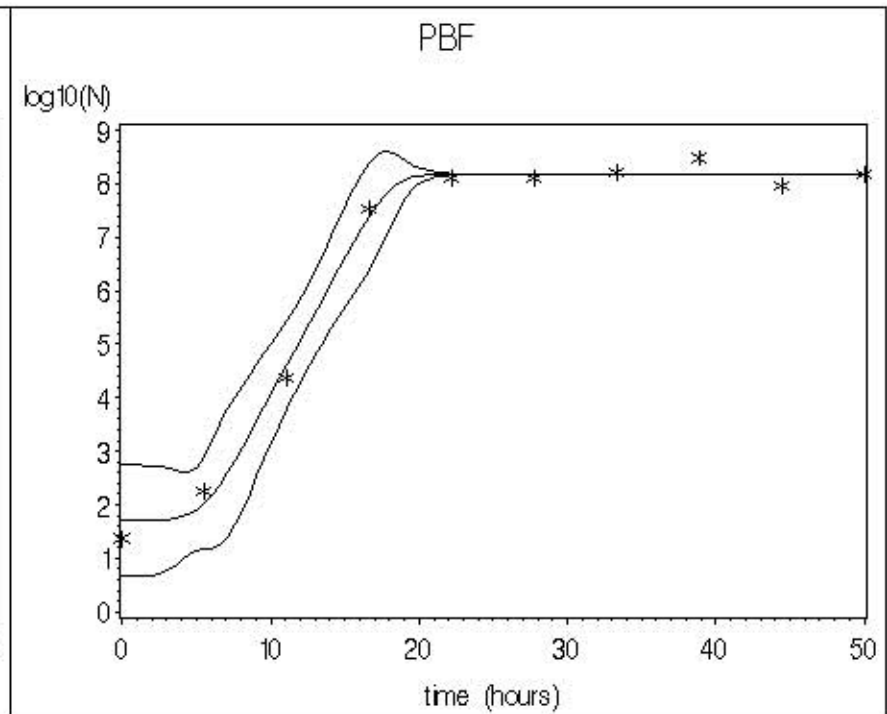
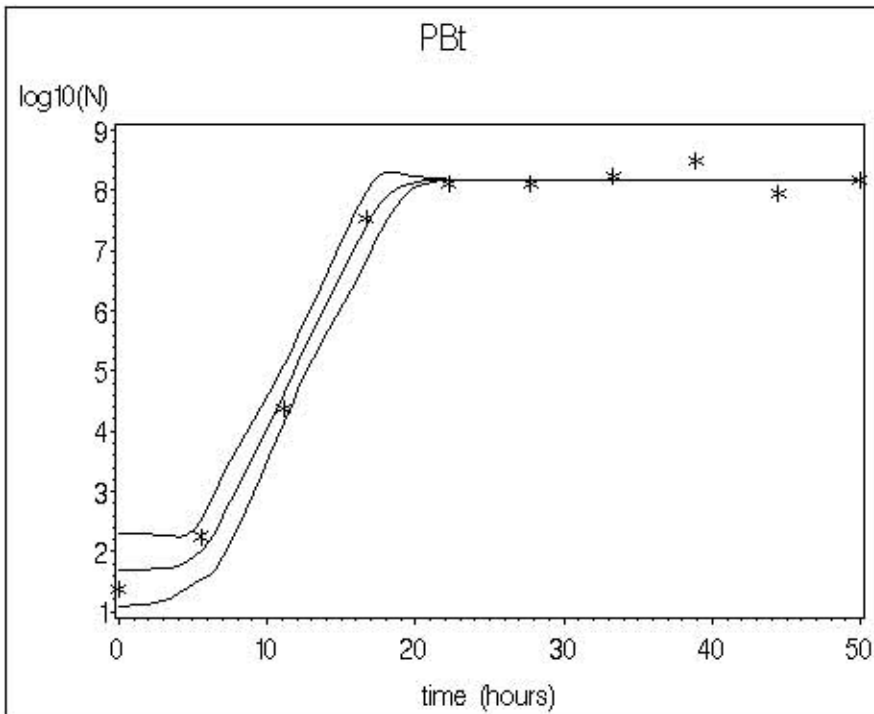
For Peer Review Only

1  
2  
3  
4  
5  
6 Fig. 1: The four bands for the Baranyi-Roberts model for one **simulated**  
7 data set (crosses stand for the simulated data). The values of the band areas  
8 (calculated with procedures indicated at the end of Subsection 3.1) are:  $\mathcal{A}(PB_t) =$   
9  $21$ ;  $\mathcal{A}(PB_F) = 36$ ;  $\mathcal{A}(PB_B) = 24$ ;  $\mathcal{A}(PB_X) = 42$ .

10  
11  
12  
13 Fig. 2: The four bands for the Baranyi-Roberts model for one real data set  
14 (crosses stand for the real data). The values of the band areas are:  $\mathcal{A}(PB_t) = 70$ ;  
15  $\mathcal{A}(PB_F) = 111$ ;  $\mathcal{A}(PB_B) = 98$ ;  $\mathcal{A}(PB_X) = 166$ .

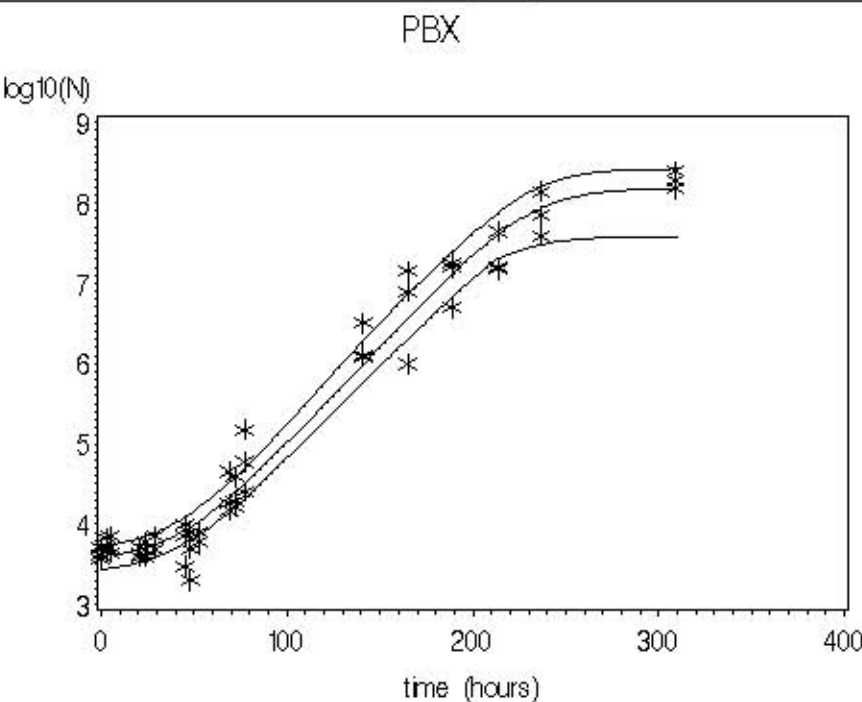
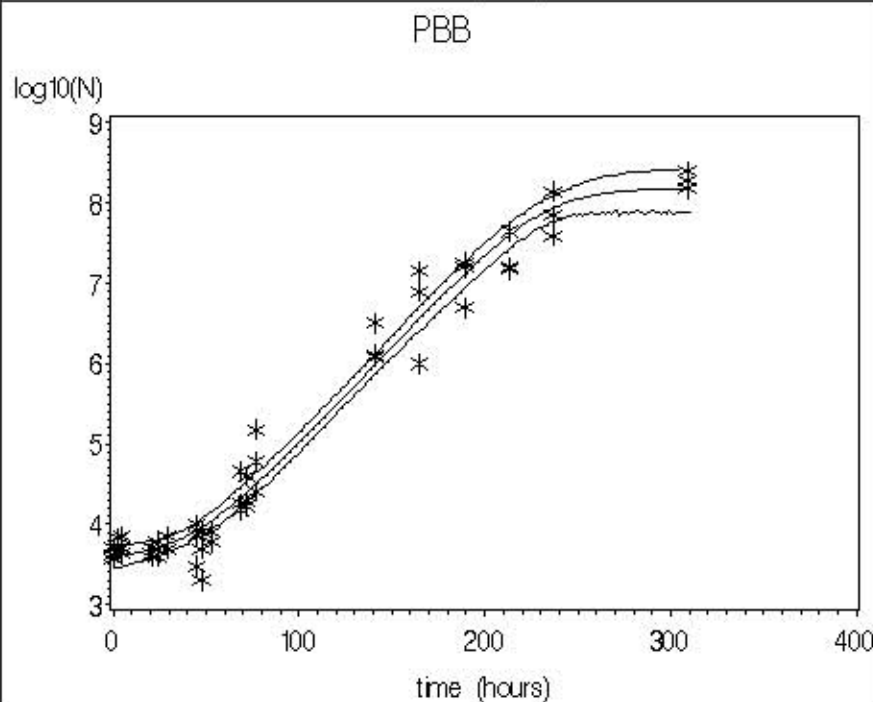
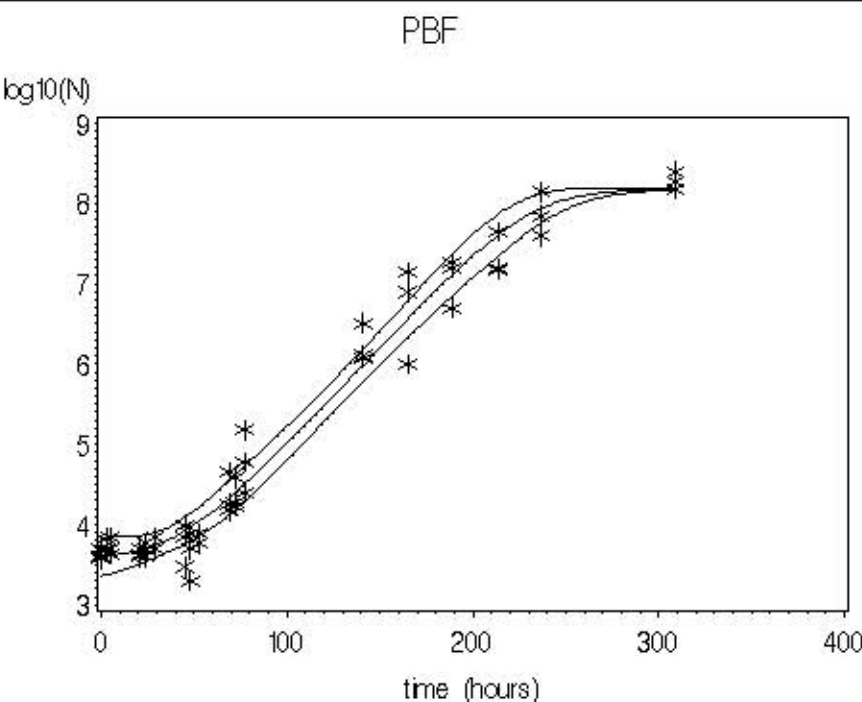
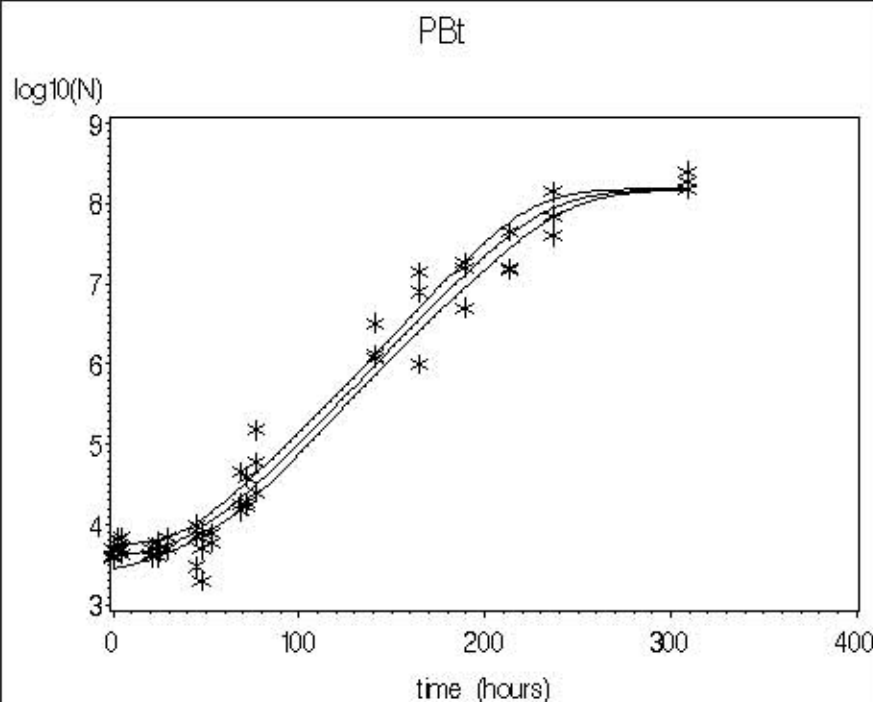
16  
17  
18  
19  
20  
21  
22  
23 Fig. 3. The four bands for the **Coroller** model for one **simulated** data  
24 set (crosses stand for the simulated data). The values of the band areas are:  
25  $\mathcal{A}(PB_t) = 7.82$ ;  $\mathcal{A}(PB_F) = 13.97$ ;  $\mathcal{A}(PB_B) = 8.90$ ;  $\mathcal{A}(PB_X) = 13.38$ . It should  
26 be noted that days appear on the abscisses, but the parameters are given in the  
27 text for the time in hours.

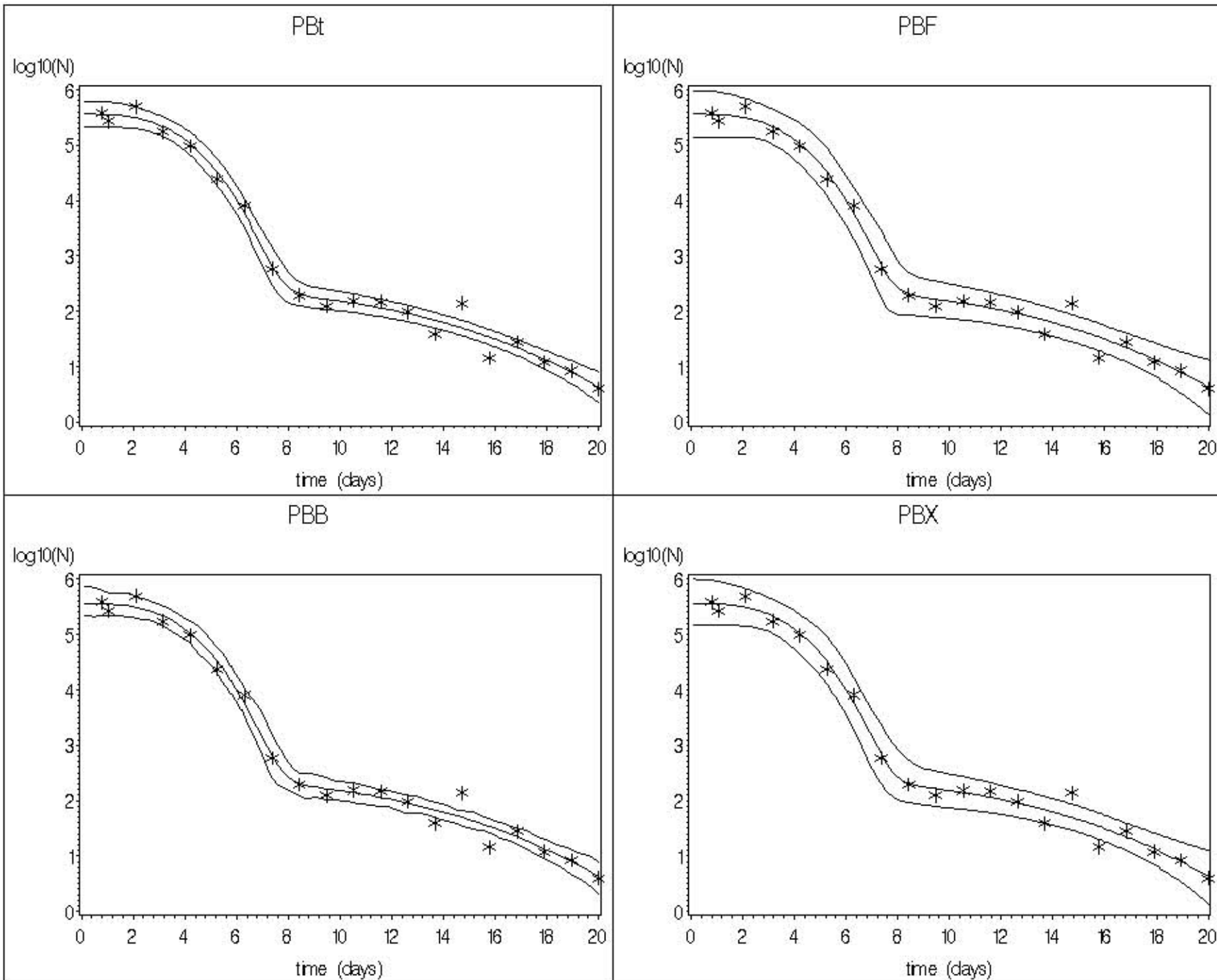
28  
29  
30  
31  
32 Fig. 4: The four bands for the Coroller model for one real data set (crosses  
33 stand for the real data). The values of the band areas are:  $\mathcal{A}(PB_t) = 9$ ;  $\mathcal{A}(PB_F) =$   
34  $15.78$ ;  $\mathcal{A}(PB_B) = 9.33$ ;  $\mathcal{A}(PB_X) = 16.54$ .



1  
2  
3  
4  
5  
6  
7  
8  
9  
10  
11  
12  
13  
14  
15  
16  
17  
18  
19  
20  
21  
22  
23  
24  
25  
26  
27  
28  
29  
30  
31  
32  
33  
34  
35  
36  
37  
38  
39  
40  
41  
42  
43  
44  
45  
46  
47  
48  
49

1  
2  
3  
4  
5  
6  
7  
8  
9  
10  
11  
12  
13  
14  
15  
16  
17  
18  
19  
20  
21  
22  
23  
24  
25  
26  
27  
28  
29  
30  
31  
32  
33  
34  
35  
36  
37  
38  
39  
40  
41  
42  
43  
44  
45  
46  
47  
48  
49





1  
2  
3  
4  
5  
6  
7  
8  
9  
10  
11  
12  
13  
14  
15  
16  
17  
18  
19  
20  
21  
22  
23  
24  
25  
26  
27  
28  
29  
30  
31  
32  
33  
34  
35  
36  
37  
38  
39  
40  
41  
42  
43  
44  
45  
46  
47  
48  
49

1  
2  
3  
4  
5  
6  
7  
8  
9  
10  
11  
12  
13  
14  
15  
16  
17  
18  
19  
20  
21  
22  
23  
24  
25  
26  
27  
28  
29  
30  
31  
32  
33  
34  
35  
36  
37  
38  
39  
40  
41  
42  
43  
44  
45  
46  
47  
48  
49

